Susceptibility of Human Oral Squamous Carcinoma Cells (OSCC) H103 and H376 cell lines to Retroviral OSKM mediated reprogramming

Nalini Devi Verusingam [1] , **Swee Keong Yeap** [2] , **Huynh Ky** [3] , **Ian C Paterson** [4] , **Suan Phaik Khoo** [5] , **Soon Keng Cheong** [1, 6] , **Alan HK Ong** [Corresp., 1] , **Tunku Kamarul** [7]

1 Faculty of Medicine and Health Sciences, Universiti Tunku Abdul Rahman, Selangor, Malaysia

2 Institute of Bioscience, Universiti Putra Malaysia, Selangor, Malaysia

3 College of Agriculture and Applied Science, Cantho University, Vietnam

4 Department of Oral Biology & Biomedical Sciences, Faculty of Dentistry, Universiti Malaya, Kuala Lumpur, Malaysia

5 School of Dentistry, International Medical University, Kuala Lumpur, Malaysia

6 MAKNA Cancer Research Institute, Kuala Lumpur, Malaysia

7 Tissue Engineering Group, National Orthopaedic Centre of Excellence for Research and Learning, Department of Orthopaedic Surgery, Faculty of Medicine, University Malaya, Kuala Lumpur, Malaysia

Corresponding Author: Alan HK Ong
Email address: onghk@utar.edu.my

Although numbers of cancer cell lines have been shown to be successfully reprogrammed into induced pluripotent stem cells (iPSCs), reprogramming Oral Squamous Cell Carcinoma (OSCC) to pluripotency in relation to its cancer cell type and the expression pattern of pluripotent genes under later passage remain unexplored. In our study, we reprogrammed and characterised H103 and H376 oral squamous carcinoma cells using retroviral OSKM mediated method. Reprogrammed cells were characterized for their embryonic stem cells (ESCs) like morphology, pluripotent gene expression via quantitative real-time polymerase chain reaction (RT-qPCR), and immunofluorescence staining, embryoid bodies (EB) formation and directed differentiation capacity. Reprogrammed H103 (Rep-H103) exhibited similar ESCs morphologies with flatten cells and clear borders on feeder layer. Reprogrammed H376 (Rep-H376) did not show ESCs morphologies but grow with a disorganized morphology. Critical pluripotency genes Oct4, Sox2 and Nanog were expressed higher in Rep-H103 against the parental counterpart from passage 5 to passage 10. As for Rep-H376, Nanog expression against its parental counterpart showed a significant decrease at passage 5 and although increased in passage 10, the level of expression was similar to the parental cells. Rep-H103 exhibited pluripotent signals (Oct4, Sox2, Nanog and Tra-1-60) and could form EB with the presence of three germ layers markers. Rep-H103 displayed differentiation capacity into adipocytes and osteocytes. The OSCC cell line H103 which was able to be reprogrammed into an iPSC like state showed high expression of Oct4, Sox2 and Nanog at late passage and may provide a potential iPSC

model to study multi-stage oncogenesis in OSCC.

1 **Susceptibility of Human Oral Squamous Carcinoma Cells (OSCC) H103 and H376 cell**
2 **lines to Retroviral OSKM mediated reprogramming**

4 Nalini Devi Verusingam[a], Swee Keong Yeap[b], Huynk Ky[c], Ian Charles Paterson[d], Suan Phaik
5 Khoo[e],Soon Keng Cheong[a,f],Han Kiat Ong[a], Tunku Kamarul[g]
6
7
8 [a] Faculty of Medicine and Health Sciences, Universiti Tunku Abdul Rahman, Selangor,
9 Malaysia.
10 [b] Institute of Bioscience, Universiti Putra Malaysia, Selangor, Malaysia.
11 [c] College of Agriculture and Applied Science, Cantho University, Vietnam.
12 [d] Department of Oral Biology & Biomedical Sciences, Faculty of Dentistry, University Malaya,
13 Kuala Lumpur, Malaysia.
14 [e] School of Dentistry, International Medical University, Kuala Lumpur, Malaysia.
15 [f] MAKNA Cancer Research Institute, Kuala Lumpur, Malaysia.
16 [g] Tissue Engineering Group, National Orthopaedic Centre of Excellence for Research and
17 Learning, Department of Orthopaedic Surgery, Faculty of Medicine, University Malaya, Kuala
18 Lumpur, Malaysia.

21 *Corresponding author at Universiti Tunku Abdul Rahman, Malaysia

22 Email address: onghk@utar.edu.my

30

31

32

33

34

35

36

37

38

39   **Introduction**

40

41   Oral cancer is the sixth most common malignancy worldwide and is more prevalent in the

42   developing than developed countries (Warnakulasuriya, 2009). More than 90% of oral cancer

43   cases are classified as Oral Squamous Cell Carcinoma (OSCC) which is a malignant epithelial

44   cancer that arises from oral keratinocytes (Scully & Bagan, 2009). As there are no reliable

45   diagnostic markers and early stage OSCC is asymptomatic, patients with OSCC are often

46   presented for treatment with advanced stage cancer resulting in a poor prognosis.

47   (Warnakulasuriya, 2009; Markopoulos, Michailidou & Tzimagiorgis, 2010)

48   In spite of the advancement in molecular based detection of cancer stages (Bose et al.,

49   2012; Rhandawa & Archaraya, 2015), the underlying biological mechanisms that take place

50   within the OSCC progression have not been well established. Existing models for OSCC study

51   derived from xenograft of primary tumours have been problematic as *in-vitro* studies have

52   resulted in low percentage of cell number and induced mutations with prolonged culture.

53   Furthermore, human cell models of OSCC from tumour cell lines generally can only mimic the

54   advanced tumour state which does not allow the different stages of cancer to be monitored and

55   studied (Shirako et al., 2015). Hence, these unresolved issues necessitate an approach to

56   establish human cancer models that recapitulate OSCC progression.

57   Originally, induced pluripotent stem cells (iPSCs) were established from adult human

58   somatic stem cells through the transient expression of Yamanaka'sOct4, Sox2, KLf4 and c-Myc

59   (OSKM) transcription factors reprogramming technology (Takahashi &Yamanaka., 2007)and

60   used as a promising stem cell source to overcome ethical and immune rejection issues that often

61 surfaced when using human Embryonic Stem Cells (hESCs) (Yamanaka, 2007).Subsequent

62 studies demonstrated that reprogrammed cancer cells were able to exhibit pluripotent capacity

63 and differentiation tendency, which were distinct from that of their parental cells with much of

64 the observable changes owing to epigenetic effects of reprogramming(Miyoshi et al.,

65 2009;Carette et al., 2010;Mahalingam et al., 2012; Gandre-babbe et al., 2013; Kim et al., 2013;

66 Zhang et al., 2013; Choong et al. 2014;Koga et al., 2014; Kotini et al., 2015; Lee et al.,

67 2015).Interestingly, while the majority of the reprogrammed cancer cells showed either lower or

68 a loss of tumorigenicity, Carette et al., 2010& Gandre-babbe et al.,2013   indicated a re-

69 establishment of the oncogenic dominance over the pluripotent cell phenotype when the

70 reprogrammed cell types were differentiated into hematopoietic lineage cells and Kim and

71 colleagues, 2013 showed that the reprogrammed human pancreatic cancer cells were able

72 recapitulate its cancer progression from early to late stage of cancer development upon

73 differentiation. In contrast, MCF-7 breast cancer cell line which was reprogrammed via

74 retroviral-OSKM method, failed to show distinct pluripotent signals and was unable to

75 differentiate into 3 primary germ layers but displayed instead, a typical cancer stem cell (CSC)

76 phenotype (Corominas-Faja et al., 2013). These reprogrammed phenotypes of cancer cells have

77 made the study of cancer development and underlying cellular systems more feasible, much of

78 which were not previously encountered from any available cancer models especially in

79 addressing cancer progression, discovery of cancer specific biomarkers and more effective

80 therapy (Lang, Shi & Chin, 2013;Lee et al., 2015;Kim & Zaret, 2015).

81

82   To the best of our knowledge, no studies have previously reported on the reprogramming

83 of OSCC cancer cells and therefore in the present study, we examined the susceptibility of two

84 OSCC cell lines to be reprogrammed into pluripotency and their respective pluripotent gene

85 expression patterns.

86

87

88 **Materials and Methods**

89

90 *Cell Culture*

91   Human Oral Squamous Cell Carcinoma cell lines (OSCC), H103 (STNMP Stage I) and

92 H376 (STNMP StageIII), obtained from Prof Ian Patterson, University Malaya, Kuala Lumpur,

93 Malaysia. Cell lines were cultured in DMEM/F12 supplemented with 10% fetal bovine serum

94 (FBS) (Gibco/Invitrogen, USA), Hydrocortisone (0.5 ug/ml) (Sigma-Aldrich, USA) at $37°C$ in

95 the presence of 5% CO2. Reprogrammed OSCC cells were maintained in conditioned hESC

96 medium consisting DMEM/F12 (Gibco/Invitrogen, USA), supplemented with 20% knock-out

97 serum replacement (Gibco/Invitrogen, USA), 0.1 mM nonessential amino acids

98 (Gibco/Invitrogen, USA), 4 mM L-glutamine (Sigma-Aldrich, USA), 10 ng/mL fibroblast

99 growth factor (bFGF) (Invitrogen, USA) and 0.1 mM 2-mecaptoethanol (Sigma-Aldrich, USA).

100 The medium was changed every 48hours.

101

102 *Retrovirus Production and Infection*

103   Retroviral vectors were produced via packaging cell lines, 293FT cell lines (human

104 embryonal kidney cells) (Thermo Fisher Scientific, USA) using the Yamanaka Factors – (Oct4,

105 Sox2. Klf4, c-Myc). Vectors, pMX-based retroviral h*Oct4* (Plasmid 17217) (Addgene, USA),

106 h*Sox2* (Plasmid 17218) (Addgene, USA), h*Klf4* (Plasmid 17219) (Addgene, USA), h*c-Myc*

107   (Plasmid 17220) (Addgene, USA), retroviral gag–pol packaging plasmid (Plasmid 8449)

108   (Addgene, USA), VSV-G expression plasmid (Plasmid 8454) (Addgene, USA) and pMX-GFP

109   (Cell Biolabs, USA) used in this experiments were provided by Dr. Shigeki Sugii, DUKE-NUS

110   Graduate Medical School, Singapore. Human embryonal kidney cell lines were plated at 3.6 x

111   10^6 (70% − 80% confluency) one day before transduction. The packaging cell lines were then

112   transfected   with   Retro-GFP/OSKM   vectors   along   with   the   transfection   reagent

113   LIPOFECTAMINE 2000 (Life Technologies, USA) according to the manufacturer's protocol.

114   The supernatant was collected at 48hours of post-transfection and filtered with PVDF filtered

115   (45uM) (Merck Milipore, USA). Polybrene (0.5ul/ml from 10mg/ml) was then added into the

116   supernatant containing Retroviral Vectors to enhance the transduction efficiency within the

117   target cell types. Presence of selection marker, green fluorescent protein (GFP) in H103 and

118   H376 were counted manually using the cell count option in ImageJ program.

119

120   *Retroviral Infection and iPSCs Cell Generation*

121   Human Oral Squamous Carcinoma Cells (H103 and H376) were seeded at 7.5 x

122   10^4cells/well on 6 well plates, 24 hours before transduction. Equal amounts of supernatant

123   containing each of the four retroviruses were collected and mixed prior to transduction of OSCC

124   cell lines. Infected cells were incubated overnight. The medium was changed at 24hours of post-

125   infection to H103 and H376 specific medium. Transduced cancer cells were then subjected to

126   spinfection at1 hour and 30 minutes (32°C) before placing the plates into a hypoxic incubator

127   (5% O_2). At day 3 post infection, OSCC cell lines were harvested by trypsinization and re-plated

128   with 1 x 10^4 cells/well on 6 well plates containing irradiated Mouse Embryonic Feeder Layer

129   (MEF) (GlobalStem, USA). After 24 hours, the medium was replaced with hESCs medium.

130 Fifteen days after transduction, formed colonies were picked up and transferred onto a new

131 mouse embryonic fibroblast (MEF) feeder layer (GlobalStem, USA). These colonies were

132 propagated at least up to five passages before being subjected to pluripotency characterization.

133

134

135

136 *Gene Expression Assessment in OSCC- Induced Pluripotent Stem Cells (iPSCs)*

137   Ribonucleic acid (RNA) was extracted from parental H103 and H376 and respective

138 reprogrammed counterparts using RNeasy Mini Kit (Qiagen, Germany) according to the

139 manufacturer's protocols. Total RNA was then converted into complementary deoxyribonucleic

140 acid (cDNA) via reverse transcription (QuantiTech Reverse Transcriptase Kit).The fluorescent

141 signals from each sample were plotted against cycle numbers which represented the

142 accumulation of product over the duration of the quantitative real-time PCR (qRT-PCR)

143 experiment. Quantitative real-time PCR amplification efficiency generated with primers

144 (Supplementary Table 1) were optimized using hESC, a commonly used gold standard for

145 pluripotency characterization. Beta-actin (ACTB) was used as a house keeping gene in this

146 experiment. Briefly, the condition used in this experiment comprises initial denaturation at 95°C

147 for 15 minutes, followed by 40 cycles of denaturation at 94°C for 30 seconds with annealing at

148 60°C for 30 seconds and extension at 72°C. Following qRT-PCR, fluorescence data collection

149 was performed during extension. Real-time PCR was performed with iQ5 Bio-Rad qPCR

150 machine (Bio-Rad, USA) using Quantitect Sybr Green PCR Master Mix (Qiagen, Germany). iQ5

151 Optical System Software, Version 2.0 was used for the analysis.

152

153 *Immunofluorescense Staining*

154   Cells were fixed using 4% v/v paraformaldehyde (Sigma-Aldrich, USA), washed three

155 times with PBS containing 1% BSA and permeablized using Perm Buffer (BD Biosciences,

156 USA) for 15 minutes at room temperature (Intracellular markers). After permeabilization, cells

157 were blocked with PBS containing 1% BSA for 1 hour at room temperature after the blocking

158 solution was removed and cells were washed three times with PBS. Cells were then incubated

159 with conjugated antibodies in PBS containing 1% BSA overnight at 4°C. Antibodies used were at

160 1:50 dilution factor for Oct4-PE (BD Biosciences, USA), Sox2-PE (BD Biosciences, USA)

161 Nanog-ALexa Fluor 488 (BD Biosciences, USA), and Tra-1-60-PE (BD Biosciences, USA).

162 After the overnight incubation, cells were washed three times with PBS and stained with DAPI

163 ANTIFADE GOLD (Invitrogen, USA) prior to viewing under Zeiss Imager A.1 Fluorescence

164 Microscope (Carl Zeiss, Germany).

165

166 *Embryoid Bodies (EB's) Formation*

167   Rep-H103 cells were seeded onto ultra-low attachment plates (Corning) containing

168 commercialize embryoid bodies medium (Milipore, USA). Transferred cells were grown in

169 suspension for 8 days. The medium was consistently changed every 2–3 days up to 8 days

170 without disrupting the EBs. EBs formed were carefully collected for immunofluorescence

171 staining to determine the presence of three germ layers specific markers (Ectoderm: OTX2,

172 Sox1; Endoderm: Sox17, Gata4; Mesoderm: Brachyury) according to the manufacturer's

173 instructions (Human Three Germ Layer 3-Color Immunostainining Kit) (R&D Systems, USA).

174 Stained cells were observed under Zeiss Imager A.1 Fluorescence Microscope (Carl Zeiss,

175 Germany).

176

177   *Directed Differentiation of Human H103 iPSCs like Cells*

178   Since H103 cell line is of the ectoderm and endoderm lineage (Jones & Klein, 2013),

179   reprogrammed H103 was subjected to directed differentiated into adipocytes and osteocytes

180   which is of the mesoderm lineages in order to access its differentiation potential.

181

182   *Osteogenic Assay*

183   Osteogenic differentiation medium (ODM) (Erenpreisa & Cragg, 2013) was used to

184   induce mineralization or osteogenesis in reprogrammed H103. IPSC-like cells were plated on

185   gelatine coated six-well plates and cultured in 3ml of ODM consisting 90% DMEM/F12

186   (Gibco/Invitrogen, USA), 10% FBS (Gibco/Invitrogen, USA) supplemented with 10nM

187   dexamethasone (Sigma-Aldrich, USA), 20mM β-glycerol phosphate (Sigma-Aldrich, USA), and

188   50μM L-ascorbic acid (Sigma-Aldrich, USA). The medium was changed every 2-3 days. After

189   21 days of incubation at 37°C, 5% CO_2, cells were stained in Alizarin Red for visualization of

190   calcium deposits. Stained cells were then evaluated under Eclipse TS100 inverted microscope

191   (Nikon, Japan) and images were captured for analysis. Presence of mineralized osteoblasts

192   indicated bright orange-red precipitate.

193

194   *Adipogenic Assay*

195   Colonies plated on gelatine coated six-well plates and were cultured in 3ml of adipogenic

196   differentiation medium (ADM) (Erenpreisa & Cragg, 2013)per well. ADM consist of 90%

197   DMEM/F12 (Gibco/Invitrogen, USA), 10% FBS (Gibco/Invitrogen, USA) supplemented with

198   0.5μM dexamethasone, 0.5 μM isobuthylmethylxanthine and 50μM indometacin. The medium

199   was changed every 2-3 days. After 21 days of incubation at 37°C, 5% CO_2, cells were stained in

200   Oil Red O for visualization of lipid droplets. Stained cells were then viewed under Eclipse

201   TS100 inverted microscope (Nikon, Japan) and images were captured for analysis. Mature

202   adipocytes containing intracellular lipid vesicles were stained bright red.

203

204   *Statistical Analysis*

205   Statistical data analysis was carried out with Paired t-Tests to compare the quantitative

206   outcome of parental, reprogrammed counterparts at passage 5 and reprogrammed counterparts at

207   passage 10 of H103 and H376 cell lines using SPSS, Software version 22.0. All tests were

208   conducted at 95% confidence level and all data were presented as mean ± standard error of mean

209   SEM. The differences were considered significant at $P<0.05$.

210   **Results**

211   *Transfection efficiencies in oral squamous Cells carcinoma cell lines*

212   Green Fluorescence Protein (GFP) serves as an internal control and used for evaluating

213   transduction efficiency. Uptake of vector pMX-GFP was tested using the highly transfectable

214   human embryonic kidney cells (293FT) (Supplementary Figure 1).Subsequently, transduction

215   efficiencies were examined in OSCC cell lines using vector pMX-GFP (16.5μg) which encodes

216   for green fluoresecent protein signals to confirm the uptake of transgenes prior to OSKM

217   transduction. GFP signals were detected in H103 and H376 at 48 hours confirming the uptake of

218   transgenes (Fig 1A). The transduction efficiency of 75.50% ± 1.52 and 38.20% ± 0.60 obtained

219   from H376 and H103 cells respectively showed an almost 2-fold increase in H376(Fig 1B).

220   Negative control was performed to access the potential influence of reprogramming on the

221   viability of the cells (Supplementary Figure 2).

222

223   *Reprogramming of oral squamous cell carcinoma cell lines*

224   Clones were picked approximately two weeks after transduction (Fig. 2A) in both H103

225   and H376 cells. Distinct morphological patterns and changes were observed between the parental

226   cancer cells and their reprogrammed counterparts (Fig. 2B i-iii & Fig 2Ci-iv). Only Rep-H103

227   clones were able to be passaged above passage 5 (Fig. 2B-iv) while clones derived from Rep-

228   H376 differentiated at passage 2 onwards and were unable to sustain iPS-like cell morphology

229   (Fig. 2C-v). Although higher GFP transfection capacity was achieved in H376, stable clones

230   were successfully generated only from H103 cell line as these clones were able to be expanded

231   up to passage 20 and still maintained an ESC-like morphology (Fig. 2B iv-v). Morphologies of

232   all derived clones from H103 are highly distinct from its parental cells with clear borders on

233   mouse embryonic fibroblast feeder layer, high nucleus to cytoplasmratio and the colonies

234   displayed small cells morphology with spaces between them (Fig. 2B iv-v).

235

236   *Differential Gene Expression*

237   Overall, the expressions of endogenous Oct4, Sox2 in Rep-H103 cells were much higher

238   than that of Rep-H376. However, suppression of Klf4 and c-Myc was seen in both

239   reprogrammed cells (Fig. 3). Pluripotent marker expression levels of the reprogrammed cells

240   relative to the parental counterparts which were quantified using qRT-PCR (Fig. 3A) showed

241   down-regulation of Oct4 expression in rep-H103 at passage 5 but increased with a 2.80 fold

242   change at passage 10. Expression of Sox2 (Fig. 3B) showed gradual up-regulation in Rep-H103

243   at passage 5 and passage 10 with 55 and77 fold change respectively. Oncogenic Klf4 (Fig 3C)

244   gene expression in reprogrammed H103 was significantly down regulated upon reprogramming

245 and the level of expression maintained throughout passage 5 and passage 10. Similar gene

246 expression pattern as Klf4 was observed in c-Myc gene (Fig 3D) but at a much lower expression

247 level. Nanog expression was also up-regulated gradually across passage 5 with 2.84 fold change

248 to passage 10 with 7.07 fold change relatively to its parental counterpart (Fig 3E).

249   In the case of Rep-H376, Oct4 expression showed an initial reduction at passage 5 of-

250 4.35 fold change but was up-regulated at passage 10 with 1.07 fold change (Fig 3A). Gradual

251 increase of Sox2expression (Fig 3B) from passage 5 to passage 10 was observed in Rep-H376, a

252 similar pattern to that of Rep-H103. Down-regulation of Klf4 expression was observed at

253 passage 5 but slightly increased from -3.13 fold change to -1.89 respectively at passage 10 (Fig

254 3C). Expression of c-Myc was almost not detected with -14.29 fold change at passage 5 and -100

255 at passage 10 (Fig 3D). Nanog expression was found reduced in Rep-H376 at passage 5 with -

256 1.79 fold change and showed little increase at passage 10 with 1.86 fold change (Fig. 3E).

257

258 *Expression of Pluripotency Associated Transcription Factors*

259   Rep-H103 continuously proliferated as adherent, flat colonies under feeder conditions

260 and captured satisfactory pluripotent signals from real-time PCR analysis compared to

261 reprogrammed H376. Therefore, successfully Rep-H103 cells were characterised further for its

262 pluripotency protein expression via immunofluorescence analysis. Rep-H103 expressed the

263 pluripotency markers of Oct4, Sox2, Nanog and Tra-1-60 indicating a distinct difference

264 between H103 derived iPS-like cells (Fig. 4A)over its parental cancer cell line (Fig. 4B).

265

266 *Differentiation: Embryoid Body Formation*

267   Three dimensional (3D) sphere-shaped structures in suspension culture formed within a

268   week in EB specific medium. At day 8, EBs were then evaluated for the presence of three germ

269   layers via immunofluorescence staining. EBs was also induced from parental cell line of H103 to

270   serve as control (Fig. 5A-i). Rep-H103 showed morphologically compact round borders EB (Fig.

271   5A-ii).   As, H103 cell line was derived from both ectodermal and endodermal lineage

272   expressions signals from these two lineages were expected to be detected in EBs from both the

273   parental and the reprogrammed counterpart(Fig. 5B-i and 5B-ii). However, mesoderm (Fig. 5B-

274   iii) expression was only detected in EBs derived from Rep-H103 indicating cross lineage

275   differentiation ability of the rep-H103 upon reprogramming into an IPS-like cell.

276

277

278

279   *Directed Differentiation Assay*

280   Crystal formation was observed during the osteogenesis process whereby the volume of

281   the matrix mineralization increased during the 21 days of incubation as indicated from the

282   Alizarin Red S stained calcium deposits (Fig. 6A-ii). In addition, tiny vesicles containing lipid

283   droplets had formed in the cytoplasm of the cells after 21 days of incubation. The accumulation

284   of lipid droplets was stained positive with Oil Red O staining (Fig. 6A-iv).

285

286   **Discussion**

287   Overall, different responses towards retroviral-OSKM mediated reprogramming were

288   observed in two different grade OSCC cell lines (H103-STNMP Stage I and H376-STNMP

289   Stage III). Rep-H103 exhibit ESCs like morphology, are distinguishable from the parental cell

290   line and generated H103 iPS-like cells could undergo *in-vitro* expansion more than 20 passages.

291   The ESC-like morphological changes in Rep-H103 corresponded to other reprogrammed cancer

292   cell lines including chronic myeloid leukemia (CML) cancer cell line (KBM7 cells) (Carette et

293   al., 2010), lung cancer cells (Mahalingam et al., 2012), liver cancer cells (Zhang et al.,

294   2014)melanoma cells (Lin et al., 2008) and osteosarcoma (Zhang et al., 2013; Choong et al.,

295   2014). On the other hand, reprogrammed H376 tended to differentiate into its original phenotype

296   and the ESC-like features were no longer observable after passage 2 (Fig. C-v).

297   Although Rep-H103 cell had successfully acquired pluripotent ectopic expressions and

298   sustained its pluripotency potentiality, it possessed lower GFP transgene uptake efficiency as

299   compared to that of Rep-H376. (Fig. B).This feature is consistent with a previous reported study

300   in which, reprogramming of four different osteosarcoma cell lines (Saos-2, MG-63, U-2 OS and

301   G-292) via Retroviral-OSKM mediated system demonstrated that U-2 OS cell line which was

302   highly responsive to GFP transduction, eventually lost its pluripotency capacity upon

303   reprogramming and could not be maintained in prolonged *in-vitro* culture. Presence of various

304   intrinsic factors between the osteosarcoma cancer cell lines was hypothesized to contribute to

305   multiple responses towards reprogramming (Choong et al., 2014).As such, depending on the cell

306   type, uptake of OSKM transgenes may not necessarily be correlated with transduction efficiency.

307   Reprogramming resistance was observed in H376 cell line in which the expressions of

308   key pluripotent genes were insignificant and the ESC-like morphological features eventually

309   diminishes with subsequent passage. Reprogramming roadblocks contributed by diverse

310   molecular properties and biophysical nature of the cell type could result in inefficient

311   reprogramming (Vierbuchen & Wernig, 2012). Notably, the tumour suppressor gene, p53 which

312   safeguards the cellular genome integrity was shown to lower reprogramming efficiency and

313   kinetics by removing DNA damaged cells at the early stages of the reprogramming stepwise

314   process via apoptosis (Vierbuchen & Wernig, 2012; Spike & Wahl, 2011). Although both H103

315   and H376 harbours the mutant p53 gene, H376 carries a p53 gene; a nonsense mutation and

316   expresses the truncated form of the protein which basically do not show any detectable mutant

317   p53 expression (Yeudal et al., 1995). Despite the fact that the mutated form of p53 gene may

318   provide a more favourable condition for reprogramming cancer cells (Ebrahimi, 2015;

319   Vierbuchen & Wernig, 2012; Spike & Wahl, 2011), the presence rather than the absence of the

320   mutant p53 expression has been reported to enhance reprogramming efficiency (Sarig et al.,

321   2010; Tapia & Scholer, 2010) as in the case of H103 which was able to maintain its pluripotent

322   features under prolonged passage. Furthermore, it has been shown that TGF- β triggers

323   epithelial-mesenchymal transition (EMT) (Ebrahimi, 2015) and the presence of transforming

324   growth factor beta-I (TGF- β) signal transduction was previously reported to be among the root

325   causes of roadblocks in reprogramming(Li et al., 2010). Moreover, successful reprogramming

326   towards pluripotency was shown to be facilitated by mesenchymal-to-epithelial transition (MET)

327   followed by suppression of epithelial-to mesenchymal transition (EMT) regulation (Chen, Han &

328   Pei, 2012). Paterson and colleagues determined the effect of transforming growth factor beta-I

329   (TGF-β) in OSCC H-series cell lines in which H376 cell line was shown to be more responsive

330   to TGF- β than H103 (Paterson et al., 1995). As such, H376 may potentially harbour higher EMT

331   activity which makes it more resistance towards reprogramming.

332   It was previously showed that extensive passaging enhances the reprogramming process

333   (Chin M. H., et al, 2009) in which the hierarchical pluripotency gene activation takes place in a

334   gradual manner upon prolong *in-vitro* passaging (Shan Z.Y., et al, 2014). Notably, in our study,

335   down-regulation of Oct4 in P5 for rep-H103may indicate that its expression was not fully

336   activated at the initial phase at P5 but its expression was more distinct at a later phase at P10

337   whereby more stable expression of pluripotent genes are expected to occur within the

338   reprogramming process. Nevertheless, the fundamental pluripotency regulators (Oct4, Sox2 and

339   Nanog) in Rep-H103 were expressed at higher levels than that of Rep-H376 at both passage 5

340   and passage 10. We observed that Nanog expression indicated a distinct difference between the

341   two cell types and their susceptibility towards reprogramming. The interactions between Oct4,

342   Sox2 and Nanog had been demonstrated via mutagenesis *in-vitro* assay and *in-vivo* functional

343   study described previously in which suppression of Oct4 and Sox2 expression respectively

344   decreases the promoter activity of Nanog (Rodda et al., 2005). Furthermore, the deficiency in

345   Nanog expression results in partially reprogrammed cells which are unable to shift into

346   pluripotency state due to impaired regulation of pluripotency network (Festuccia et al., 2013).

347   Such was the case as reported by Miyoshi et al., (2009) in which gastrointestinal cell lines

348   selected for reprogramming were shown to express low level of Nanog mRNA, but gradually

349   acquired significant up-regulation of Nanog expression upon reprogramming with four

350   pluripotent transcription factors. In our studies, further evidence of pluripotency was confirmed

351   on successfully Rep-H103 via the immunofluorescence staining for common intracellular (Oct4,

352   Sox2, Nanog) and extracellular (Tra-1-60) pluripotent markers, which were used in pluripotent

353   stem cells characterization. All intracellular and extracellular pluripotent markers were detected

354   on reprogrammed H103 indicating pluripotency expressions were achieved at the protein level.

355   As Klf4 is known to act either as a tumour suppressor gene or an oncogene, depending on

356   the need of the tumour cells and the types of cancer (Evans & Liu, 2008) and c-Myc is a crucial

357   oncogene that confers immortality in cancer cells via a shift from senescence state to oncogenic

358   progression (Erenpreisa & Cragg, 2013), these transcription factors have been highly implicated

359   in influencing cancer progression. The down-regulation pattern of oncogenic gene expression,

360   namely c-Myc and Klf4 in both H103 and H376 were also observed in reprogrammed human

361   osteosarcoma cells (Zhang et al., 2013). Furthermore, when teratoma formations were assessed,

362   it was found that the parental cancer cells formed tumour at a faster rate than that of the

363   reprogrammed counterpart which exhibited a reduced aggressive cancer phenotype. Down-

364   regulation of both c-Myc and Klf4 in reprogrammed OSCC suggests reprogramming may initiate

365   an epigenetic reversal process on the oncogenic gene networks in cancer cells and this

366   phenomenon could be utilized as a therapeutic strategy for treatment of OSCC.

367   The differentiation potential demonstrated that Rep-H103 which initially originated from

368   ectoderm and endoderm lineage (Jones & Klein, 2013), portrays its capability of differentiating

369   into osteocytes and adipocytes which are of the mesoderm lineage. The ability to differentiate

370   into all three germ layers has been commonly observed in successfully reprogrammed cells

371   including iPS-like cancer cells (Carette et al., 2010; Rizzino, 2013) and is crucial in generating

372   post-IPSCs to unravel the underlying tumorigenesis development of the specific cancer.

373   Reprogrammed OSCC cell lines (H103 and H376) were used as a cancer-specific model

374   to provide a conceptual study on the cells ability to be reprogrammed into a pluripotent state and

375   their pluripotent characteristics at the in-vitro level.   Since our study involves a stage I (H103)

376   and stage III (H376) OSCC cell lines, the findings obtained does not address the effect of

377   reprogramming on stage IV OSCC (the final stage in the STNMP classification) and the

378   outcomes of the pluripotent signals at the in-vivo level. The next phase of the study is being

379   planned to address the current limitation of the findings.

380   In summary, the maintenance of stem cell like morphology and pluripotent expressions

381   upon reprogramming was only observed in rep-H103 cells. This may be due to the differences in

382   the inherent genetic make-ups between H103 and H376 cell lines, which determined their

383   capacity to be reprogrammed into iPS-like cells. Our findings indicated a typical up-regulation

384   pattern of endogenous transcription factors – Oct4, Sox2 and Nanog in the reprogrammed H103

385   cell. However, down-regulation of oncogenes, c-Myc and Klf4 was observed in both Rep-H103

386   and Rep-376 cells, As such, the OSCC reprogrammed cells are potential models for further

387   studies on cancer progression in OSCC, by enabling access to cancer properties from the initial

388   tumour initiation to the later malignant/metastatic states as well as models for the discovery of

389   novel anti-cancer drugs.

390

391   **Acknowledgments**

392   We would like take this opportunity to thank Assistant Professor Dr. Shigekii Sugii from DUKE-

393   NUS Graduate Medical School, Singapore, for sharing his iPSCs knowledge and technology

394   with us. We would also like to thank Dr. Teoh Hoon Koon, Teh Hui Xin and Choong Pei Fen

395   who sequenced the plasmids.

396

397

398   **References**

399   **Bose P, Klimowicz AC, Kornaga E, Petrillo SK, Matthews TW, Chandarana S,**
400   **Magliocco AM, Brockton NT, Dort JC.**2012. Bax expression measured by AQUA analysis
401   is an independent prognostic marker in oral squamous cell carcinoma. *BMC Cancer***12**(1):1.
402

403   **Brana I, Siu LL.**2012. Locally advanced head and neck squamous cell cancer: treatment
404   choice based on risk factors and optimizing drug prescription.*Annals of*
405   *Oncology***23**(10):x178-x185.
406

407   **Carette JE, Pruszak J, Varadarajan M, Blomen VA, Gokhale S, Camargo FD, Wernig**
408   **M, Jaenisch R, Brummelkamp TR**. 2010. Generation of iPSCs from cultured human
409   malignant cells. *Blood*. **115**(20):4039-42.
410

411 **Chen J, Han Q, Pei D.**2012. EMT and MET as paradigms for cell fate switching. *Journal of*
412 *molecular cell biology***4**(2):66-69.
413
414 **Choong PF, Teh HX, Teoh HK, Ong HK, Choo KB, Sugii S, Cheong SK, Kamarul**
415 **T.**2014.Heterogeneity of osteosarcoma cell lines led to variable responses in reprogramming.
416 *International Journal of Medical Science***11**:1154-60.
417
418 **Corominas-Faja B, Cufí S, Oliveras-Ferraros C, Cuyàs E, López-Bonet E, Lupu R,**
419 **Alarcón T, Vellon L, Manuel Iglesias J, Leis O, Martin A.**2013.Nuclear reprogramming
420 of luminal-like breast cancer cells generates Sox2-overexpressing cancer stem-like cellular
421 states harboring transcriptional activation of the mTOR pathway. *Cell Cycle***12**(18):3109-
422 3124.
423
424 **Ebrahimi B.**2015. Reprogramming barriers and enhancers: strategies to enhance the
425 efficiency and kinetics of induced pluripotency. *Cell Regeneration***4**(1):1.
426
427 **Erenpreisa J, Cragg MS.**2013. Three steps to the immortality of cancer cells: senescence,
428 polyploidy and self-renewal. *Cancer Cell Int***3**(1):92.
429
430 **Evans P M, Liu C.**2008. Roles of Krupel-like factor 4 in normal homeostasis, cancer and
431 stem cells. *Acta Biochim Biophys Sin (Shanghai)***40**(7):554-64.
432
433 **Festuccia N, Osorno R, Wilson V, Chambers I.**2013. The role of pluripotency gene
434 regulatory network components in mediating transitions between pluripotent cell states.
435 Current Opinion in Genetics & Development 23(5):504-11.
436
437 **Gandre-Babbe S, Paluru P, Aribeana C, Chou ST, Bresolin S, Lu L, Sullivan SK,**
438 **Tasian SK, Weng J, Favre H, Choi JK.**2013.Patient-derived induced pluripotent stem cells
439 recapitulate hematopoietic abnormalities of juvenile myelomonocytic leukemia. *Blood*
440 **121**(24):4925-9.
441
442 **Jones KB, Klein OD.**2013. Oral epithelial stem cells in tissue maintenance and disease: the
443 first steps in a long journey. *International Journal of Oral Sciences***5**(3):121-9.
444 **Kim J, Hoffman JP, Alpaugh RK, Rhim AD, Reichert M, Stanger BZ, Furth EE,**
445 **Sepulveda AR, Yuan CX, Won KJ, Donahue G**. 2013.An iPSC line from human
446 pancreatic ductal adenocarcinoma undergoes early to invasive stages of pancreatic
447 progression. *Cell Reports***3**(6):2088-99.
448 **Kim J, Zaret KS.** Reprogramming of human cancer cells to pluripotency for models of
449 cancer progression. 2015. *The EMBO Journal***34**(6):739-47.
450
451 **Koga C, Kobayashi S, Nagano H, Tomimaru Y, Hama N, Wada H, Kawamoto K,**
452 **Eguchi H, Konno M, Ishii H, Umeshita K.** 2014. Reprogramming using microRNA-302

improves drug sensitivity in hepatocellular carcinoma cells. *Annals of Surgical Oncology***21**(4):591-600.

Kotini AG, Chang CJ, Boussaad I, Delrow JJ, Dolezal EK, Nagulapally AB, Perna F, Fishbein GA, Klimek VM, Hawkins RD, Huangfu D.2015. Functional analysis of a chromosomal deletion associated with myelodysplastic syndromes using isogenic human induced pluripotent stem cells. *Nature biotechnology***33**(6):646-55.

Lang JY, Shi Y, Chin YE.2013. Reprogramming cancer cells: back to the future. *Oncogene***32**(18):2247-8.

Lee DF, Su J, Kim HS, Chang B, Papatsenko D, Zhao R, Yuan Y, Gingold J, Xia W, Darr H, Mirzayans R. 2015.Modeling Familial Cancer with Induced Pluripotent Stem Cells. *Cell***161**(2):240-54.

Lee SY, Park HR, Cho NH, Choi YP, Rha SY, Park SW, Kim SH.2013. Identifying genes related to radiation resistance in oral squamous cell carcinoma cell lines. *International Journal of Oral and Maxillofacial Surgery***42**(2):169-76.

Li R, Liang J, Ni S, Zhou T, Qing X, Li H, He W, Chen J, Li F, Zhuang Q, Qin B.2010.A mesenchymal-to-epithelial transition initiates and is required for the nuclear reprogramming of mouse fibroblasts. *Cell stem cell***7**(1):51-63.

Lin SL, Chang DC, Chang-Lin S, Lin CH, Wu DT, Chen DT, Ying SY.2008.Mir-302 reprograms human skin cancer cells into a pluripotent ES-cell-like state. *RNA***14**(10):2115–2124.

López-Otín C, Blasco MA, Partridge L, Serrano M, Kroemer G.2013.*The Hallmarks of Aging*. Cell *153*(6):1194-1217.

Mahalingam D, Kong CM, Lai J, Tay LL, Yang H, Wang X.2012. Reversal of aberrant cancer methylome and transcriptome upon direct reprogramming of lung cancer cells. *Sci Rep***2:**592.

Markopoulos AK, Michailidou EZ, Tzimagiorgis G. 201o. Salivary markers for oral cancer detection. *The open dentistry journal***27**;4(1).

Miyoshi N, Ishii H, Nagai KI, Hoshino H, Mimori K, Tanaka F, Nagano H, Sekimoto M, Doki Y, Mori M.2009. Defined factors induce reprogramming of gastrointestinal cancer cells. *PNAS***107**(1):40-5.

O-charoenrat P, Pillai G, Patel S, Fisher C, Archer D, Eccles S, Rhys-Evans P.2003.Tumour thickness predicts cervical nodal metastases and survival in early oral tongue cancer. *Oral oncology***39**(4):386-390.

495 **Paterson IC, Patel V, Sandy JR, Prime SS, Yeudall WA.**1995. Effects of transforming
496 growth factor beta-1 on growth-regulatory genes in tumour-derived human oral
497 keratinocytes. *British journal of cancer***72**(4):922.

498

499 **Petersen PE.**2005. Strengthening the prevention of oral cancer: the WHO perspective.
500 *Community Dental Oral Epidemiology***33**(6):397-9.

501

502 **Rhandawa V, Archaraya V.**2015.Integrated network analysis and logistic regression
503 modeling identify stage-specific genes in Oral Squamous Cell Carcinoma. *BMC Medical*
504 *Genomics***8**(1):39.

505

506 **Rizzino A.**2013. Concise Review: The Sox2-Oct4 Connection: Critical Players in a Much
507 Larger Interdependent Network Integrated at Multiple Levels. *Stem Cells***31**(6):1033-9.

508

509 **Rodda DJ, Chew JL, Lim LH, Loh YH, Wang B, Ng HH, Robson P.** 2005.
510 Transcriptional Regulation of Nanog by OCT4 and SOX2. *Journal of Biological*
511 *Chemistry***280:**24731-24737.

512

513 **Sarig R, Rivlin N, Brosh R, Bornstein C, Kamer I, Ezra O, Molchadsky A, Goldfinger**
514 **N, Brenner O, Rotter V.**2010.Mutant p53 facilitates somatic cell reprogramming and
515 augments the malignant potential of reprogrammed cells.*The Journal of Experimental*
516 *Medicine***207**(10):2127–2140.

517

518 **Scully C, Bagan J.**2009. Oral squamous cell carcinoma overview. Oral Oncology **45**(4-
519 5):301-8.

520

521 **Shenoi R, Devrukhkar V, Sharma BK, Sapre SB, Chikhale A.** 2012. Demographic and
522 clinical profile of oral squamous cell carcinoma patients: A retrospective study. *Indian*
523 *journal of cancer***49**(1):21.

524

525 **Shirako Y, Taya Y, Sato K, Chiba T, Imai K, Shimazu Y, Aoba T, Soeno**
526 **Y.**2015. Heterogeneous tumor stromal microenvironments of oral squamous cell carcinoma
527 cells in tongue and nodal metastatic lesions in a xenograft mouse model. *Journal of Oral*
528 *Pathology of Medicine***44**(9):656-68.

529

530 **Spike BT, Wahl GM.**2011. P53, stem cells, and reprogramming tumor suppression beyond
531 guarding the genome. *Genes & cancer***2**(4):404-19.

532

533 **Takahashi K, Tanabe K, Ohnuki M, Narita M, Ichisaka T, Tomoda K, Yamanaka**
534 **S.**2007. Induction of pluripotent stem cells from adult human fibroblasts by defined factors.
535 *Cell***131**(5):861-72.

536

537 **Tapia N, Schöler HR.**2010. P53 connects tumorigenesis and reprogramming to
538 pluripotency. *The Journal of experimental medicine***207**(10):2045-2048.

539

540   **Vierbuchen T, Wernig M.**2012. Molecular roadblocks for cellular
541   reprogramming. *Molecular cell***47**(6):827-838.
542

543   **Warnakulasuriya S**.2009."Global epidemiology of oral and oropharyngeal cancer."*Oral
544   oncology***45**(4):309-316.
545

546   **Yamanaka, S**. 2007. Strategies and new developments in the generation of patient-specific
547   pluripotent stem cells. *Cell Stem Cell*. **1**: 39–49.
548

549   **Yeudall WA, Paterson IC, Patel V, Prime SS.**1995. Presence of human papillomavirus
550   sequences in tumour-derived human oral keratinocytes expressing mutant p53. *European
551   Journal of Cancer Part B: Oral Oncology* **31**(2):136-143.

552   **Zhang DM, Li JJ, Yan P, Hu JT.**2014.Establishment and identification of
553   induced pluripotent stem cells in liver cancer patients. *Asian Pac J Trop Med***7**(4):253-6.
554

555   **Zhang P, Zhang Z, Zhou X, Qiu W, Chen F, Chen W.**2006. Identification of genes
556   associated with cisplatin resistance in human oral squamous cell carcinoma cell line. *BMC
557   Cancer***6**(1):224.
558

559   **Zhang X, Cruz FD, Terry M, Remotti F, Matushansky I.**2013.Terminal differentiation
560   and loss of tumorigenicity of human cancers via pluripotency-based reprogramming.
561   *Oncogene***32**(18):2249-60.
562

563

564

565

566

567

568

Figure 1

Transduction Efficiency of Retroviruses in OSCC

Fig 1 - (A) Oral squamous carcinoma cell lines (H103 and H376) were introduced with ecotropic pMXs retroviruses containing GFP cDNA. The upper panel shows the images of bright-field and fluorescent microscope, Zeiss Axiovert inverted microscope, original magnification: 20x. (B) The lower panel shows the percentages of cells transduced with GFP. Data are expressed as mean ± standard deviation (SD).
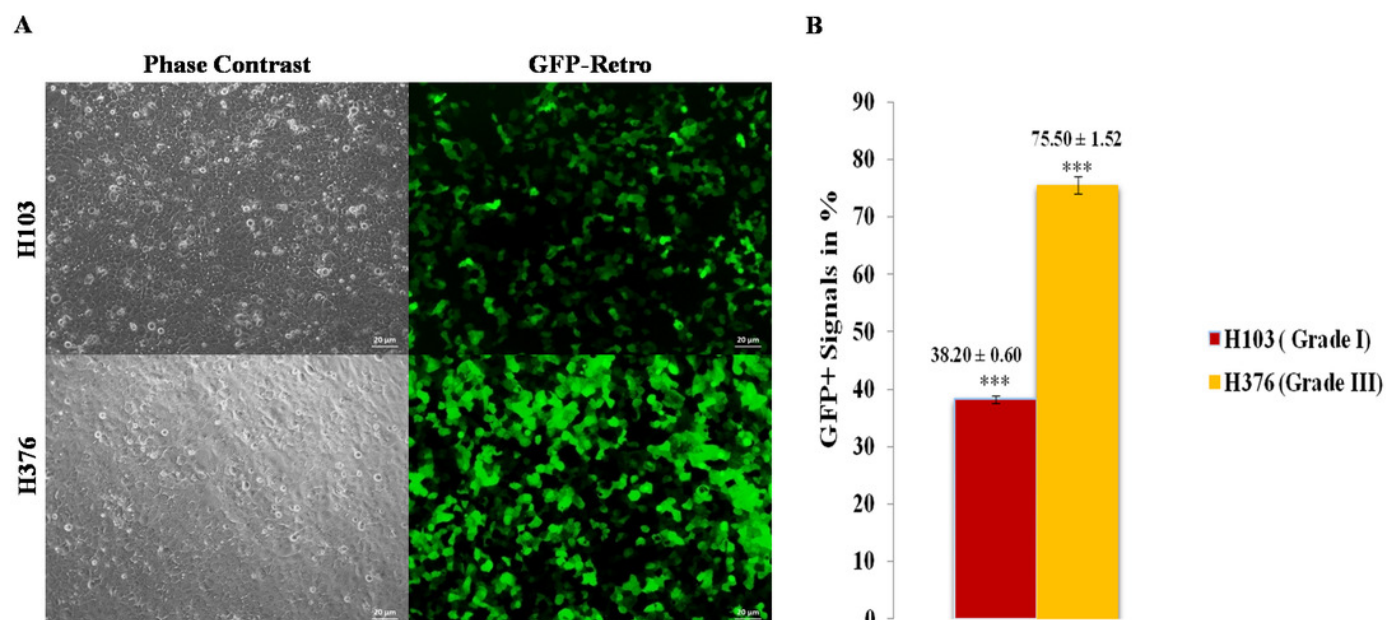
Figure 2

Induction of Pluripotent cells from OSCC

Fig 2 - (A) Timeline of iPSCs induction. (B-i) Morphology of H103. (B-ii) Morphology of transduced H103 at 24 hours post infection. (B-iii) Emergence of iPSCs like colonies from reprogrammed H103 on MEF feeder layer at day 15 (Red arrow). (B-iv-v) Images of established stable H103 iPSCs like cells at passage number 10. (C-i) Morphology of H376. (C-ii) Morphology of transduced H376 at 24 hours post infection. (C-iii) Emergence of IPSC like colonies from H376 on MEF feeder layer at day 15 (Red arrow). (C-vi) Image of iPSC like cells from H376 at P2. (C-v) Differentiated reprogrammed H376 (Red arrows), collected at P5 and P10 for real time expressions analysis.
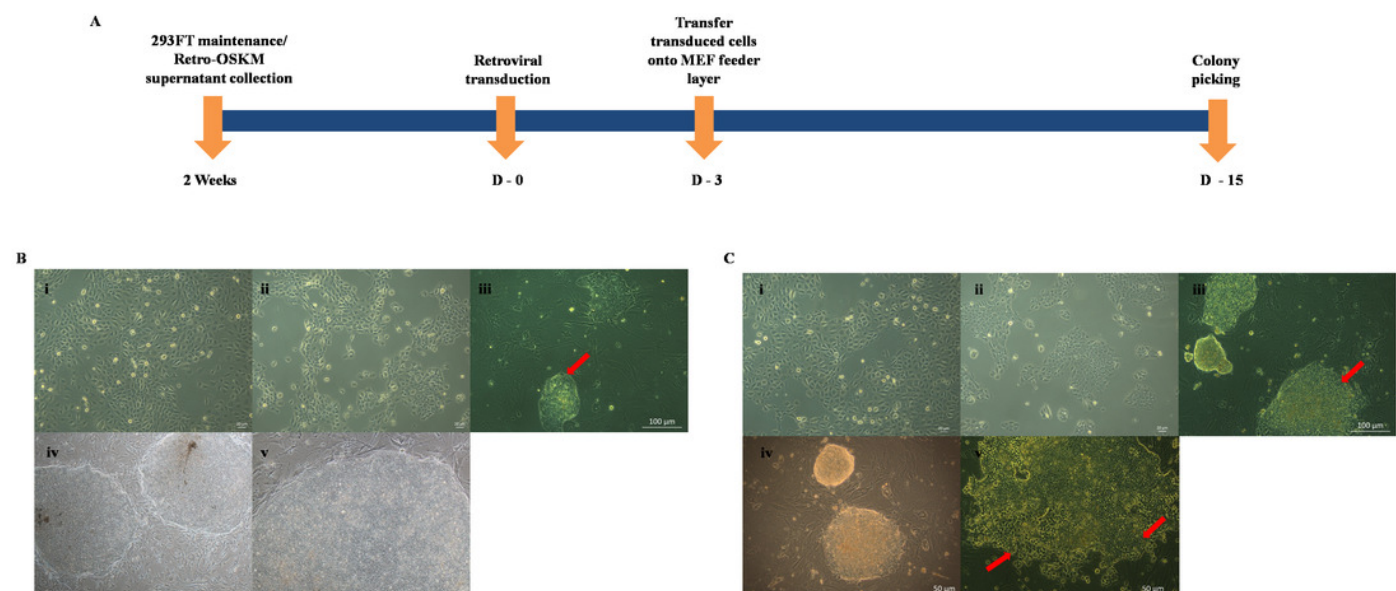
Figure 3

In-Vitro mRNA expression of pluripotent genes in reprogrammed H103 and H376 Relative to Parental (n-3)

Fig 3 - (A-E) Data presented as mean ± SEM. Statistical differences are indicated with * for P<0.05, ** for P<0.01 and *** for P<0.001 using paired t-test.
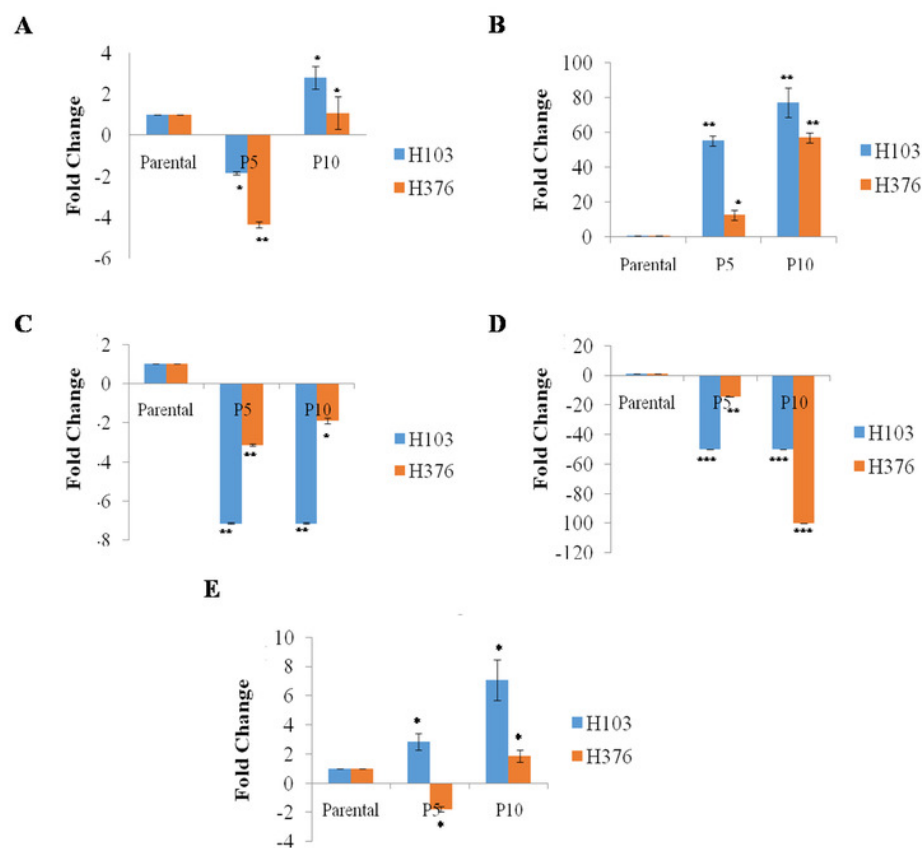
Figure 4

Expression of Pluripotent Marker

Figure 4 - (A) REP-H103 expressed markers common to pluripotent cells including OCT4, SOX2, NANOG and TRA-1-60. (B) Pluripotency markers (OCT4, SOX2, NANOG and TRA-1-60) were not expressed in parental cancer cell.
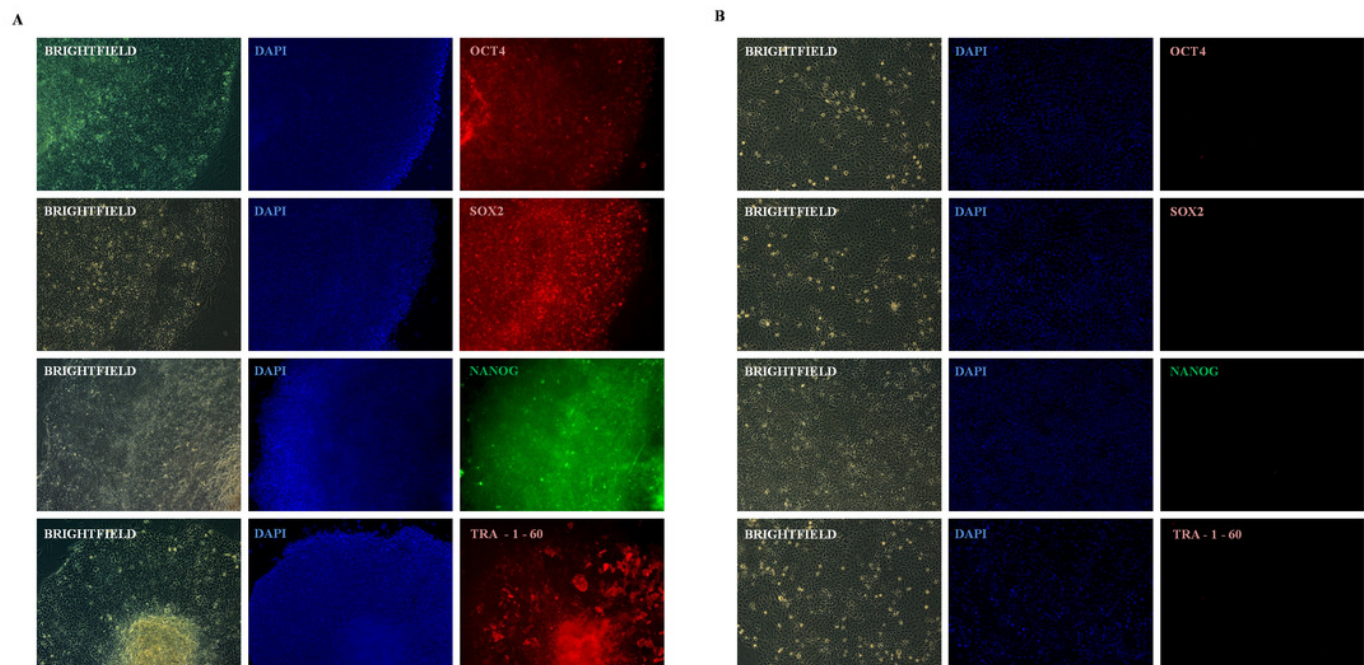
Figure 5

Embryoid bodies (EBs) formation and immunofluorescence staining

Fig 5 - Representative images of (A-i) parental H103-EB cells and (A-ii) reprogrammed H103-EB. The better showed compact structure and round borders-EB exhibited by reprogrammed H103-EB which is lack in parental H103-EB structure (Red arrow). Nikon inverted microscope, original magnification:10x. Immunostaining analysis indicates the presence of three germ layers of (B-i) ectoderm - OTX2/SOX1, (B-ii) endoderm - GATA4/SOX17 and (B-iii) mesoderm - BRACHYURY.
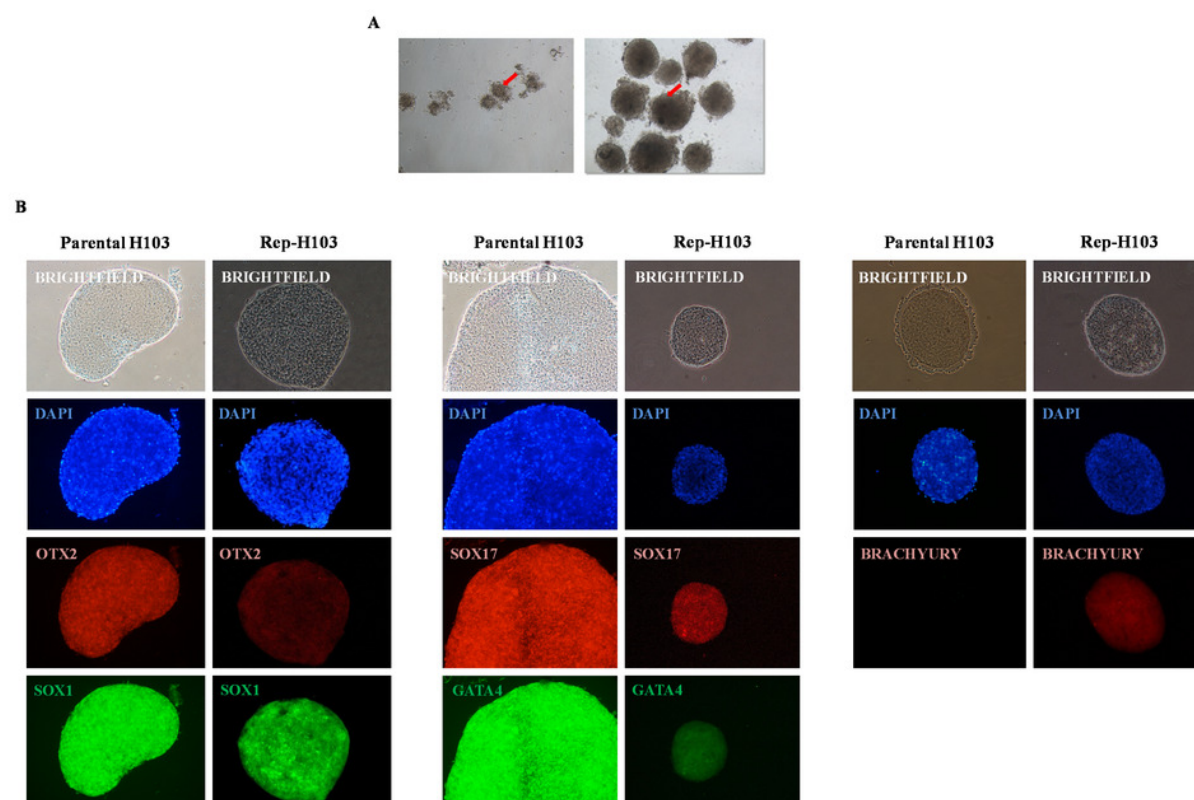
Figure 6

Directed differentiations into Osteocytes and Adipocytes

Fig 6 - (A-i) Control parental H103 cells showing negative for the Alizarin red staining (A-ii) H103 IPSCs like cells showing positive for the Alizarin red staining indicating calcium deposits (Red arrow). (A-iii) Negative staining for Oil-Red-O in control parental H103 cells. (A-iv) Adipogenesis induced lipid droplets observed red in colour stain after Oil-O-Red staining. (Red arrow) indicates the tiny lipid droplets. Nikon inverted microscope, original magnification: (A-i & ii) 10x, (A-iii & iv) 40x.